Polymer 51 (2010) 1578–1584

Contents lists available at ScienceDirect

Polymer

journal homepage: www.elsevier.com/locate/polymer

The influence of polymer morphology on the performance of molecularly imprinted polymers

Niamh Holland*, June Frisby, Eleanor Owens, Helen Hughes, Patrick Duggan, Peter McLoughlin

Pharmaceutical and Molecular Biotechnology Research Centre, Waterford Institute of Technology, Cork Road, Waterford, Ireland

ARTICLE INFO

Article history:
Received 17 April 2009
Received in revised form
9 October 2009
Accepted 13 October 2009
Available online 17 October 2009

Keywords:
Molecularly imprinted polymer
Morphology
Thermal desorption GC–MS

ABSTRACT

This is the first in-depth study examining the effect of morphology on the performance of 2-aminopyridine (2-apy) imprinted polymers. A series of polymers were prepared by varying the amount of crosslinking monomer (EGDMA) whilst the other polymer components remained constant. Physical characterisation was carried out using conventional techniques, such as nitrogen sorption porosimetry and solvent swelling studies. The use of a novel thermal desorption GC–MS technique suggested higher levels of polymer degradation with prolonged exposure to elevated temperatures for those polymers formed with lower amounts of EGDMA. The thermal desorption GC–MS profiles obtained correlated with the physical characteristics of the polymers, where higher levels of polymer bleed was found to occur with larger average pore diameters. Polymer physical characteristics were also found to correlate with the binding parameters (number of binding sites and polymer–template association energy) obtained from the Langmuir–Freundlich Isotherm (L–FI) and affinity distribution spectra (AD). The flexibility of the polymers formed from lower amounts of EGDMA combined the swelling effect of the solvents on the polymers resulted in an increase in affinity, which was both specific and non-specific in nature.

1. Introduction

The performance of molecularly imprinted polymers (MIPs) is not only dictated by the interaction of template with the functional monomer pre- and post-polymerisation on a molecular level, but also by the physical make up of the polymer on a macro level. Imprinted polymers are generally insoluble materials whose subsequent use depends on their morphology in terms of the particle shape and size and the porous texture of the material. Therefore, it is important to determine the morphology of imprinted polymers as it can effect their subsequent molecular recognition properties and/or their mode of application.

Typical polymer characterisation techniques include optical microscopy (e.g. scanning electron microscopy (SEM), transmission electron microscopy (TEM) and scanning probe microscopy (SPM) [1,2]), sorption measurements (e.g. nitrogen or mercury sorption [3,4]) and thermal analysis (e.g. differential scanning calorimetry (DSC) and thermogravimetric analysis (TGA) [5,6]). Other techniques such as swelling, FTIR and NMR analysis have also found use in characterising polymers [7,8]. The molecular recognition behaviour of MIPs is examined by analysis of polymer affinity and specificity, typically carried out in solution using equilibrium binding experiments or by HPLC analysis [9].

Recently, a technique based on thermal desorption GC–MS analysis has been presented as a novel methodology for the characterisation of MIPs [10,11]. Thermal desorption analysis involves coupling a GC–MS with a direct probe sample introduction device. The sample is exposed to a pre-determined temperature programme and the desorbed materials are transported to an MS detector where they are qualitatively analysed. The initial investigations into the use of this methodology showed how the technique could be used to follow template removal in the initial pre-treatment stage and to assess specificity and selectivity during polymer reloading. The technique also displayed sensitivity that could identify differences in polymer performance based on compositional changes.

The phenomenon of heterogeneity predominately occurs in non-covalently imprinted polymers due to the instability of the pre-polymerisation monomer–template complexes. This can be problematic as it results in the formation of a range of binding sites with varying affinities towards the template species. This heterogeneous property can limit the use of MIPs, particularly in chromatographic applications where it can lead to poor resolution and peak asymmetry [12], and it can also lead to cross-reactivity in sensors [13]. A combination of studies on pre-polymerisation complexes (by NMR, UV or FTIR spectroscopy) and analysis of the

* Corresponding author. Tel.: +353 51 302727.
E-mail address: nholland@wit.ie (N. Holland).

0032-3861/$ – see front matter © 2010 Elsevier Ltd. All rights reserved.
doi:10.1016/j.polymer.2009.10.035

heterogeneous nature of the resultant polymers can lead to the determination of an optimum composition for imprinting a specific template. This can result in maximum polymer performance in subsequent applications.

Only in recent years have post-polymerisation attempts been made to characterise the heterogeneous nature of imprinted polymers. Typically an experimental binding isotherm is generated for the imprinted polymers and it is then possible to estimate the binding behaviour of the system by fitting the experimental isotherm to various mathematical models, for example Langmuir (LI), Bi-Langmuir (Bi-LI or Scatchard), Freundlich (FI) and the hybrid Langmuir–Freundlich (L–FI) isotherms. Each of these models has their advantages and disadvantages, which are discussed in detail in review papers by Diaz-Garcia [9] and Umpleby [14]. Bi-LI is typically applied using Scatchard plots and has up until recently been the most common method for the assessment of MIPs. However, because of its limitations, including the assumption that binding occurs at either high or low affinity binding sites as opposed to a range of affinities of binding sites, a recent trend has been to use a variety of binding isotherms in polymer assessment.

An earlier study that utilised LI, FI and L–FI for polymer characterisation compared covalent and non-covalent polymers, all of which were taken from the literature [15]. The FI has been used previously to examine the binding behaviour of polymers formed using different compositions [16]. The use of the isotherms individually, or as a combination, have typically been used to identify the most appropriate model for a given template using only one polymer composition [17], a comparison of bulk and precipitation polymers [18], assessment of binding to films [19], by varying the type of functional monomer and the template used [20] or used for the assessment of the cross reactivity of an imprinted polymer [21].

L–FI is increasingly becoming the model of choice for MIP characterisation. Unlike LI and FI, L–FI is capable of simultaneously modelling the binding characteristics of imprinted polymers at both high and low concentrations for heterogeneous and homogeneous systems [9,14,15]. It has also been proven to accurately model the binding behaviour of imprinted polymers, as demonstrated by Umpleby et al. [15] who applied the model to five systems (heterogeneous and homogeneous) taken from the literature.

Affinity distribution analysis of binding sites can be carried out by surface topography characterisation [9], expectation maximisation (EM) methods [22–24] or by the generation of affinity distribution (AD) spectra [15,16,25–35]. AD spectra typically display the number of binding sites with respect to association constant of those sites. While AD spectra have found use in the assessment of imprinted polymers, the majority of those plots have been generated based on FI parameters [16,25–28,30–34], or directly by Hunstons approximation method [35–38]. Umpleby et al. are the only group, to date, to report the generation of AD spectra based on L–FI binding parameters [15].

The following study was carried out so as to characterise the morphological changes pertaining from various polymer compositions using the novel thermal desorption GC–MS technique, mentioned above, and also by using LI, FI, L–FI and AD spectra. The imprint system chosen for analysis was methacrylic acid-co-ethylene glycol dimethacrylate (MAA-co-EGDMA) selective towards 2-aminopyridine (2-apy). This system has previously been studied, both in terms of pre-polymerisation monomer–template interactions [39] and post-polymerisation selectivity towards the template and structural analogues [40–43]. However, such studies, in terms of the binding capability, have been carried out on polymers formed using only one ratio of MAA-co-EGDMA (1:30). As the performance of this system is well established it therefore acts as an ideal candidate for investigating the effect of morphology (i.e. the porous structure) on the performance of imprinted polymers. This study also allows for further investigation into the suitability of thermal desorption GC–MS for the characterisation of MIPs, and it is also the first report of the use of LI, FI, L–FI and AD spectra based on the L–FI fitting parameters in the examination of composition on polymer performance, as carried out in the solution phase. Comparisons to traditional polymer characterisation techniques, such as nitrogen sorption porosimetry and solvent swelling studies, were also made.

2. Experimental

2.1. Materials

Ethyleneglycol dimethacrylate (EGDMA) (98%), methacrylic acid (MAA) (99%), 1,1-azobis(cyclohexanecarbonitrile) (ACCN) (98%) and 2-aminopyridine (2-apy) (>99%) (all purchased from Sigma–Aldrich (Dublin, Ireland)). All solvents were of analytical grade minimum. Chloroform (Lennox Dublin, Ireland) was stored over molecular sieves (3 ∼, 3.2 mm) to maintain the absence of moisture. Polymerisation was conducted in VGA-220-241K 20 mL glass vials, which were sealed with VGA-221-510D 20 mm stoppers and 20 mm crimp seals.

2.2. Polymer synthesis

Polymers were synthesised using a previously described method [11,43].

2.3. Nitrogen sorption analysis and solvent swell ratio determination

The solvent swell ratio was determined in chloroform, acetonitrile and methanol based on a method described by Mashelkar et al. [44]. The swelling ratio (Sr) was calculated using Equation (1) [45], based on the volume of dry polymer and the volume of wet polymer. The average value of triplicate independent results were obtained.

$$\text{Swelling ratio (Sr)} = \frac{\text{volume of wet polymer}}{\text{volume of dry polymer}} \quad (1)$$

Nitrogen sorption analysis was carried out on approximately 15 mg quantities of polymer using a Gemini VI Surface Area and Pore Size Analyser (Micrometrics). One hundred and ten point adsorption/desorption isotherms were generated and the surface area of the polymers was derived from the adsorption isotherm, in the P/P_0 range < 0.3 for a six point plot, using Brunauer, Emmett and Teller (BET) analysis.

Pore analysis was carried out using the Barrett, Joyner and Halden (BJH) method [46]. Pore radii at each P/P_0 point was determined using the Kelvin equation (Equation (2)), which was corrected for multilayer adsorption using the Halsey thickness equation (Equation (3)). Differential pore volumes were generated by plotting dV/dD versus D (V is the pore volume and D is the pore diameter) [47].

$$r^k = \frac{2\sigma^{1g}\nu^1}{RT\ln(P_o/P)} \quad (2)$$

Where [48]; r^k is the Kelvin radius,

$\sigma^{1g}$is the surface tension of the liquid condensate, and,

ν^1 is the molar volume of the liquid condensate.

The Halsey thickness equation, which corrects for multilayer adsorption is given in Equation (3).

$$t = 3.55\left[\frac{-5.00}{\ln(P/P_o)}\right]^{1/3} \quad (3)$$

Where [4]; t is the thickness of the adsorbed liquid monolayer, and, 3.45 and 5.00 are empirical values.

The average value of duplicate independent results was obtained.

2.4. Thermal desorption GC–MS analysis of polymers

Thermal desorption experiments on the polymers were carried out using a Varian CP-3800 Gas Chromatograph coupled with a Varian Saturn 2000 GC/MS/MS, as previously described [10,11]. A Varian Chromatoprobe was attached to one of the temperature programmable injection ports of the GC which was connected *via* a programmable switching valve to the MS detector through a 1 m uncoated capillary column (i.d. 100 μm) housed in the GC column oven. The flow gas was CP-grade helium at 0.5 mL min^{-1} min. The programmable switching valve was used to select fractions for MS analysis or to vent fractions to waste in order to protect the MS detector from excessive exposure in the early part of the thermal treatment.

2.5. Binding analysis

Fifty mg quantities of the polymers were weighed into 10 mL volumetric flasks to which 5 mL of 0.025 mM–4.0 mM 2-apy in chloroform were subsequently added. The flasks were stoppered and equilibrated in a Stuart Scientific Orbital Incubator S150 at 25 °C for 16 h. Polymer solutions were then filtered using Omnifix 10 mL syringes fitted with OEM syringe nylon filters (0.45 μm). The quantity of reloaded binding substrate bound to the polymer, B (see Equation (4)), was determined by UV/VIS spectroscopic analysis of the post equilibrium solution at the pre-determined wavelength (approximately $\lambda_{abs} \approx 290$ nm). The average values of triplicate independent results were obtained.

$$B = T - F \quad (4)$$

Where; B is the amount of substrate bound to the polymer,
T is the initial amount of substrate added to the polymer, and,
F is the amount of free substrate in solution after equilibration.

Table 1
Linearised forms of LI, FI and L–FI [9].

Isotherm	Linearised Form	Plot	Parameters
LI	$1/B = (1/N_t a) + (1/F)$	$1/B$ versus $1/F$	$N_t = 1$/intercept, a = intercept/slope
FI	$m\log F = \log A$	$\log B$ versus $\log F$	$a = y$ intercept, m = slope
L–FI	Solver function[a]	$\log B$ versus $\log F$	Fitting coefficients- N_t, a and m.

[a] L–FI were fitted to the log–log plot of the experimental isotherms using Microsoft Excel by varying the fitting parameters to minimise the coefficient of variation (R^2) determined to 1 as described by Shimizu et al. [15].

An experimental isotherm was generated by plotting B versus F and was subsequently fit to the Langmuir (LI), Freundlich (FI) and the hybrid Langmuir–Freundlich (L–FI) isotherms LI, FI and L–FI (Equations (5), (6) and (7) respectively) as outlined in Table 1. Affinity distribution spectra were generated by fitting the L–FI binding parameters into Equation (8), using Microsoft Excel Solver function [15].

- Langmuir isotherm (LI)

$$B = \frac{N_t a F}{1 + aF} \quad (5)$$

- Freundlich isotherm (FI)

$$B = aF^m \quad (6)$$

- Langmuir–Freundlich isotherm (L–FI)

$$B = \frac{N_t a F^m}{1 + aF^m} \quad (7)$$

- Affinity distribution equation for the L–FI

$$N_i = N_t a m (1/K_i)^m x \frac{\left(1 + 2a(1/K_i)^m + a^2(1/K_i)^{2m} + 4a(1/K_i)^m m^2 - a^2(1/K_i)^{2m} m^2 - m^2\right)}{\left(1 + a(1/K_i)^m\right)^4} \quad (8)$$

Where; N_t is the total number of binding sites,
a is related to the average binding affinity K_0 *via* $K_0 = a^{1/m}$,
m is the heterogeneity index, and,

$$\log K = \log\left(\frac{1}{\left(\frac{F}{1000}\right)}\right)$$

3. Results and discussion

3.1. Nitrogen sorption analysis and solvent swell ratio determination

The sorption isotherms for the 10 mmol and 40 mmol[1] imprinted polymers are shown in Fig. 1. The 40 mmol polymers, both MIP and NIP (NIP isotherms not shown), produced Type IV isotherms, consistent with mesoporous structures, with type H3 or H4 hysteresis. The 10 mmol polymers produced isotherms similar to a Type II isotherm which is indicative of non-porous or macroporous materials. The adsorption and desorption mechanisms were similar which is usually indicative of larger pores [47]. Non closure of the loop, which was observed for all isotherms, implies incomplete removal of adsorbate from narrow pores [48].

The BET surface area and the pore data obtained are given in Table 2.

The 40 mmol polymers had a larger surface area than corresponding 10 mmol polymers. This was in agreement with previous studies where surface areas have been shown to decrease with decreasing crosslinker ratios [49]. Higher surface areas are indicative

[1] 10 mmol and 40 mmol refer to the concentration of EGDMA in the polymer formulations.

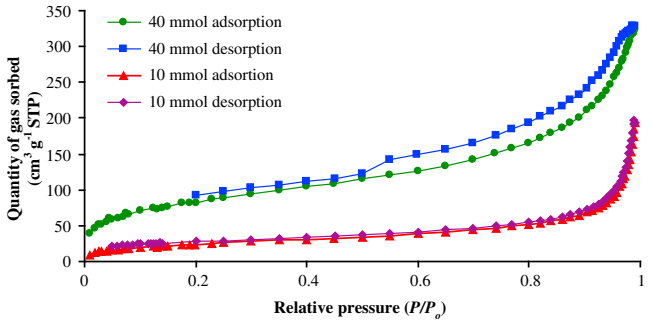

Fig. 1. Sorption isotherms for the imprinted polymers containing 40 and 10 mmol EGDMA.

of phase separation occurring at later stages of the polymerisation and the formed polymers are accompanied with smaller pore size distributions [50,51].

Similar trends in average pore volumes were observed on going from the more crosslinked polymers to the less crosslinked polymers. The pore volume distribution plots are illustrated in Fig. 2. The average pore volume for all polymers was in the mesoporous region. The 10 mmol polymers were less porous than the corresponding 40 mmol polymers as is observed by the lower pore volume in Fig. 2 and Table 2.

The polymer swelling ratios, as determined in chloroform, acetonitrile and methanol, are illustrated in Fig. 3.

Chloroform swelled the polymers to a larger extent than acetonitrile or methanol. This was expected as chloroform was the porogen and would be expected to fill the pores in accordance with polymerisation conditions. The polymers with higher surface areas had lower swell ratios. This was consistent with previous studies [44,52], swelling would be expected with lower crosslink ratios. Although the cumulative volume of pores was less for the polymers formed from lower amounts of EDGMA, the greater flexibility allowed greater solvent ingress to the pores. Thus, more of the pores may have been filled possibly causing greater expansion of the pores and the surrounding polymer network. The broader distribution of pore sizes for the 10 mmol polymers must also be considered. Corresponding MIP and NIP polymers swelled to the same degree in all of the solvents. This is in agreement with the pore volume distribution plots where solvent ingress through the pore network is expected to be similar for comparable pore distributions.

3.2. Thermal desorption GC–MS analysis of polymers

The initial pre-treatment step of thermal desorption GC–MS can be used to facilitate the removal of unreacted polymer components, as outlined in the early work utilising this technique [10,11]. Fig. 4 illustrates the pre-treatment desorption profiles attributed to EGDMA (crosslinking monomer) for the 10 mmol and 40 mmol polymers.

The NIP polymers consistently displayed higher levels of bleed, relative to corresponding imprinted polymers, across multiple analyses. Similar to the solvent swell studies, the pore structures (i.e. the pore volume distributions) would facilitate the migration of desorbed materials from within the polymer network. As the pore volume distribution profiles for MIPs and NIPs were experimentally similar (Fig. 2(a) and (b)), the pre-treatment analysis supports the earlier hypothesis that the non-imprinted polymers may not have been crosslinked to the same degree as corresponding imprinted polymers [10,11]. What must also be considered is that the average pore diameter for the NIP species was larger than MIP polymers, for both compositions. Consequently, this may also have contributed to the higher level of bleed observed from the NIP polymers as the free volume within the NIP polymers was larger thus facilitating increased levels of migration within the polymer matrix.

During the assessment of polymer affinity it was again possible to carry out a bleed composition analysis. Fig. 5 illustrates the RIC (Reconstructed Ion Chromatogram, which displays the total ion count for all ions generated in the range m/z 40–300) for 40 and 10 mmol MIPs and the profiles for 2-apy, EGDMA, MAA and chloroform (m/z 83) for the 10 mmol imprinted polymer. The RIC profile, more specifically the high level of bleed relative to the other components, would suggest possible degradation coinciding with the ramps of the temperature programme employed. There was less bleed for the 40 mmol polymer than for the 10 mmol suggesting a higher level of degradation for the latter composition.

Bleed due to EGDMA was identified during the template reloading stage, again, suggesting possible degradation. The maximum temperature reached during both the pre-treatment and reloading was 250 °C. While the pre-treatment temperature program consisted of a different temperature ramp than that used in the reloading analysis, both have the same max temperature of 250 °C. Fig. 6 visually illustrates the difference between the bleed obtained for a pre-treatment versus reloading. It was evident from analysis of the desorption profiles (Fig. 6) that a larger amount of EGDMA was displaced during the pre-treatment stage. It is presumed that the bleed in the pre-treatment stage was due to residual unreacted crosslinking monomer. As the binding capability of the polymers was shown to diminish with prolonged exposure to elevated temperatures [10], indicating possible destruction of binding sites, it is suggested that the bleed during reloading was due to degradation as opposed to removal of residual EGDMA.

3.3. Binding isotherms and affinity distribution analysis of MIPs

LI and FI displayed poorer fits (R^2) to the experimental binding data relative to L–FI (Table 3). Thus, the results discussed in this work are based on the novel application of L–FI and AD spectra on the effect of varying the amount of crosslinking monomer on the binding characteristics of 2-apy imprinted polymers.

The fitting coefficients N_t, a and m were determined using Solver function (see Table 4). For these values to be accurately obtained K_0 (average association constant) must fall within the limits $1/F_{min}$ and $1/F_{max}$ (the limits of affinity distribution). This is a pre-requisite in determining the suitability of L–FI. These values were determined by the relationships $K_{min} = 1/F_{max}$ and $K_{max} = 1/F_{min}$, where F is the concentration of free analyte in solution. As the K_0 value for all of the

Table 2
Summary of the BET surface areas and the pore data obtained for the polymers formed using 40 and 10 mmol of EGDMA.

Polymer	BET surface area ($m^2\ g^{-1}$)		Cumulative surface area of pores ($cm^3\ g^{-1}$)		Cumulative volume of pores ($cm^3\ g^{-1}$)		Average pore diameter (nm)	
	MIP	NIP	MIP	NIP	MIP	NIP	MIP	NIP
40 mmol EGDMA	293.9 (±9.9)	347.2 (±2.5)	260.9 (±20.4)	289.6 (±4.6)	0.481 (±0.025)	0.606 (±0.005)	7.4 (±0.2)	8.4 (±0.2)
10 mmol EGDMA	93.1 (±11.8)	67.1 (±0.6)	92.4 (±14.5)	64.6 (±4.9)	0.313 (±0.022)	0.225 (±0.022)	13.6 (±1.2)	14.0 (±2.4)

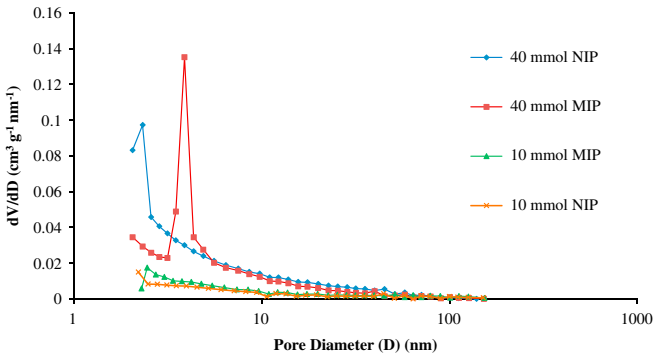

Fig. 2. Differential pore volume distributions for the polymers formed using 40 mmol and 10 mmol EGDMA.

polymers fell within these limits (coupled with the improved R^2 values) the information obtained on the binding characteristics are deemed appropriate for polymer study. The general trend observed for the average association constant, K_0, was that it decreased with decreasing EGDMA content. The reduction in K_0 may be attributed to the presence of less defined binding sites as a result of lower amounts of crosslinking monomer.

The total number of binding sites, N_t, was found to increase with deceasing EGDMA content. This trend was expected due to the increased flexibility which permitted the intrinsic sites of the polymer to become occupied, resulting in the observed overall higher capacity of the polymers. The average pore diameter decreased with increasing EGDMA amount which may have resulted in a greater sieving capability of those polymers, ultimately leading to an overall lower capacity (and number of calculated binding sites). As the initial concentration of template to monomer remained constant for all polymers there should, in theory, be an equal number of binding sites present in all of the polymers. However, applying the L–FI to the polymers indicated that this was not the case. The flexibility and various porous structures of the polymers combined with the swelling of the polymer in chloroform may have resulted in greater access within the polymer matrix. This then resulted in a higher degree of binding, which may have been both specific and non-specific in nature [11]. Therefore, while the number of sites was shown to increase with decreasing EGDMA content the values given do not account for potential non-specific binding.

The heterogeneity indices, m, for all polymers were high indicating that the polymers were approaching homogeneity. This result was unexpected as the polymers were imprinted non-covalently which typically results in heterogeneity due to the instability of the template–monomer complexes pre-polymerisation. A value of m

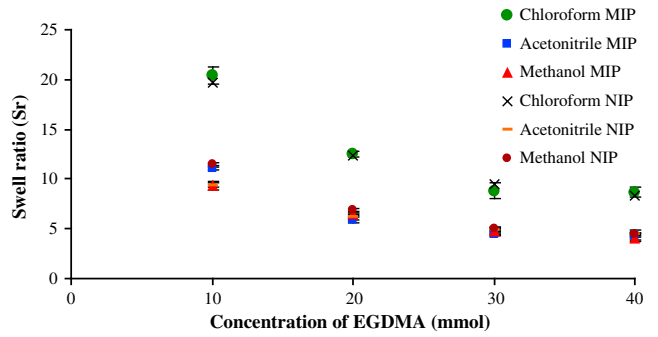

Fig. 3. Swell ratio in chloroform, acetonitrile and methanol for imprinted polymers and non-imprinted polymers.

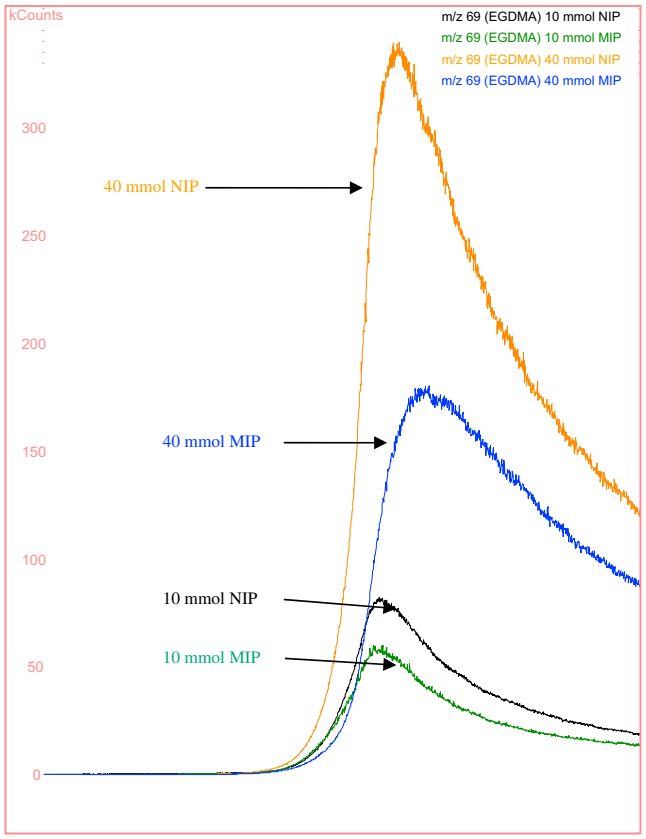

Fig. 4. Pre-treatment thermal desorption profiles obtained for the polymers formed using 40 and 10 mmol EGDMA.

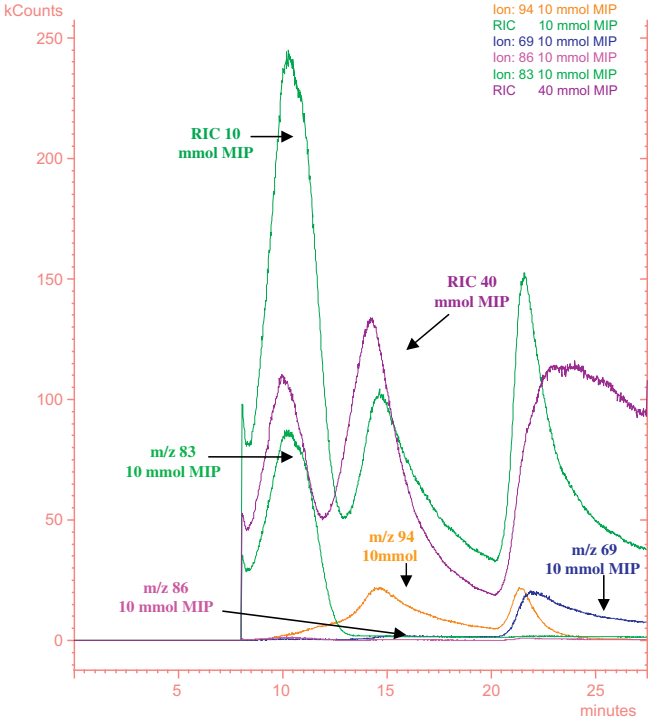

Fig. 5. RIC for the 40 and 10 mmol MIPs and the profiles for 2-apy (m/z 94), EGDMA (m/z 69) and chloroform (m/z 83) for the 10 mmol imprinted polymer.

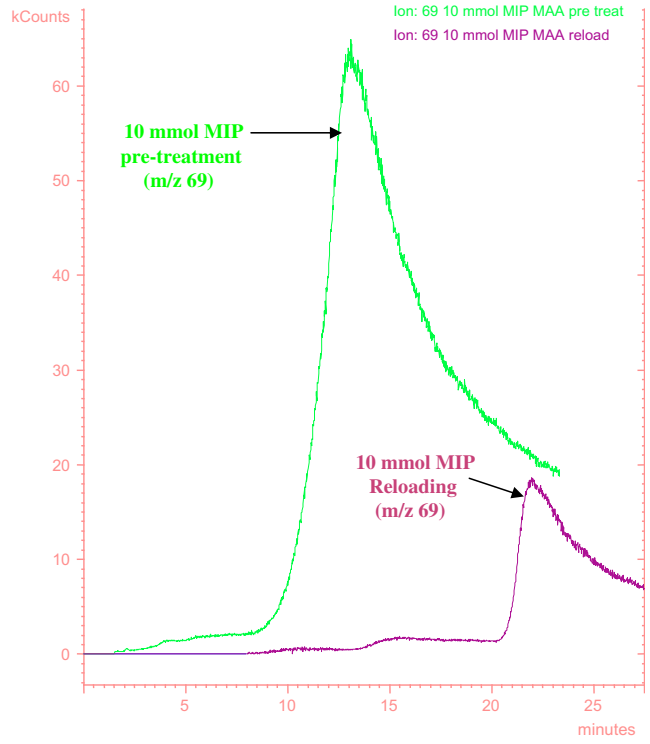

Fig. 6. Bleed attributed to EGDMA for 10 mmol imprinted polymer for pre-treatment and reloading.

Table 3
Regression (R^2) values for each MIP composition obtained from LI, FI and L–FI.

EGDMA	LI	FI	L–FI
40 (mmol)	0.936	0.921	0.892
30 (mmol)	0.921	0.927	0.968
20 (mmol)	0.578	0.851	0.868
10 (mmol)	0.754	0.919	0.921

Table 4
Binding data obtained from fitting the experimental data to the L–FI for each MIP composition.

EGDMA	N_t (μmol g^{-1})	a (mM^{-1})	m	K_0 (mM^{-1})[a]	Limits of affinity distribution (mM^{-1})[b]
40 (mmol)	88.6	0.94	0.97	0.94	0.32–28.3
30 (mmol)	136.7	0.78	0.99	0.78	0.30–35.7
20 (mmol)	259.9	0.52	1.00	0.52	0.39–52.9
10 (mmol)	281.9	0.53	0.80	0.46	0.40–84.0

[a] The average association constant $K_0 = a^{1/m}$.
[b] Limits of affinity distribution were calculated from the maximum and minimum values of F by the relationships $K_{min} = 1/F_{max}$ and $K_{max} = 1/F_{min}$, [15].

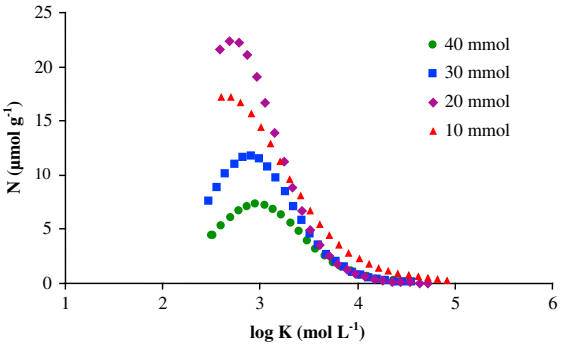

Fig. 7. Affinity distribution spectra for MIPs.

equal to one results in the L–FI reducing to the LI. The FI is inaccurate at very low concentrations of analyte [9], as a result the L–FI is also inaccurate at very low analyte amounts. The heterogeneity index values obtained may be due to the inability of the L–FI to accurately reduce to the FI at very low concentrations.

From the parameters obtained from L–FI an affinity distribution (AD) spectrum was generated for the polymer species. An AD spectrum displays the population of binding sites, N, having a particular association constant, K. For the affinity distribution spectra to be deemed accurate the K_0 value, determined from the L–FI fitting parameters, must fall within the limits of affinity distribution. As was seen in Table 4 all polymers fell within these limits. The area under the curve corresponds to the total number of binding sites.

The AD spectra for all MIPs are shown in Fig. 7 and are plotted in semi-log format. The exponentially decaying region correlates with reloading in the lower concentration region and assesses the high affinity sites. As the AD spectra shown are unimodal distributions, as opposed to only displaying the exponentially decaying region, it indicates that the polymers have been assessed in a broad concentration range and that the polymers have reached saturation. As a result more information can be gained on the type and number of binding sites. The narrow shape of the distributions indicates that the imprinted polymers are relatively homogeneous in nature, which was determined by fitting the data to L–FI.

The heterogeneity index determines the shape of the distribution where the shape broadens when m is reduced from 1 to 0. The AD spectra were clearly able to distinguish between each polymer composition.

For the 40 and 30 mmol imprinted polymers, the number of binding sites increased with decreasing EGDMA concentration, with the exception of the 10 and 20 mmol compositions. A change in the K value for the maximum number of binding sites (N_{max}) with composition change was also identified. N_{max} shifted to a lower K value with decreased EGDMA concentration, again suggesting the presence of less defined binding sites due to the potential destabilisation of the template–monomer complexes in the early stages of polymerisation. Aside from N_t, the fitting parameters a and m, as well as K_i, (refer to Equation (8)) should be

Table 5
Summary of the relationship between polymer composition and the various experimental parameters obtained. The arrow heads are pointing in the direction of the highest to lowest value for each parameter determined. For the exact values refer to the text and Tables 2–4.

EGDMA (mmol)	BET SA[a] (m^2 g^{-1})	Cumulative SA of pores (cm^3 g^{-1})	Cumulative volume of pores (cm^3 g^{-1})	Average pore diameter (nm)	Sr[b]	m/z 69 pre-treatment	m/z 69 reloading	N_t (μmol g^{-1})	K_0 (mM^{-1})	Affinity
40	↓	↓	↓	↑	↑	↓	↑	↑	↓	↑
10										

[a] SA = Surface area.
[b] Trend correct for chloroform, acetonitrile and methanol.

considered when determining the binding sites *via* AD. As these parameters are different between the two compositions different AD spectra were expected.

3.4. Summary of results

The experimental results discussed in the above sections highlight a clear link between the effect of morphology and the subsequent performance of MIPs. Through the use of numerous techniques, the physical characteristics of the polymers, such as porosity, surface area, the swell ratio in various solvents and polymer bleed, were linked to various performance related parameters i.e. the affinity of the polymers towards the template, the total number of binding sites and the binding energy. These trends are summarised in Table 5.

4. Conclusion

The investigation into the relationship between morphology and the performance of MIPs has been carried out extensively through the novel application of thermal desorption GC–MS and affinity distribution spectra generated from the L–FI fitting parameters. Correlations between the morphological characteristics of the polymers, as determined by the traditional polymer characteristion technique nitrogen sorption porosimetery, and the results obtained using thermal desorption GC–MS, the L–FI and AD spectra were identified, thus highlighting the suitability of the latter techniques as polymer characterisation methodologies.

The thermal desorption GC–MS technique is novel in terms of analysing the thermal stability/degradation properties of polymers. The initial pre-treatment stage of the methodology permits a bleed composition analysis [10,11]. Whilst other techniques such as TGA can offer a similar insight into the thermal properties of polymers, this technique is more specific as it allows identification of the various degradents. It is suggested that the technique is not applicable solely to the characterisation of imprinted polymers and that it may be used for the assessment of other polymeric materials.

The L–FI isotherm was deemed the most appropriate isotherm for analysis in the concentration range used. This was based on the improved linear regression values obtained when it was fit to the experimental data. The L–FI was sufficiently sensitive to identify changes in binding site energies with change in composition and correlations were identified between the physical properties of the polymers and the results obtained, where the total number of binding sites increased with increasing flexibility. The average binding energy of the sites decreased with decreasing EGDMA amounts. This highlights the importance of the crosslinking monomer in maintaining the fidelity of the binding sites during polymerisation. The AD spectra were a useful tool in displaying the relationship between the number of binding sites and their associated energy. This was also the first use of AD spectra based on the L–FI fitting parameters in the examination of composition on polymer performance.

Acknowledgements

Financial support from the Council of Directors, under the Technology Sector Strand 1, and the European Unions INTERREG IIIA programme is gratefully acknowledged.

References

[1] Sawyer LC, Grubb DT. In: Polymer microscopy. 2nd ed. Oxford: Chapman and Hall; 1996.
[2] Cristallini C, Ciardelli G, Barbini N, Giusti P. Macromol Biosci 2004;4:31–8.
[3] Lowell S, Shields M, Thomas M, Thommes M. Characterization of porous solids and powders: surface area, pore size and density. Dordrecht, The Netherlands: Kluwer Academic Publishers; 2004.
[4] Webb PA, Orr C. Analytical methods in fine particle technology. Micrometrics Instrument Corp; 1997.
[5] Levchik GF, Si K, Levchik SV, Camino G, Wilkie CA. Polym DegradStability 1999;65:395–403.
[6] Varghese H, Bhagawan SS, Thomas S. J Therm Anal Calorim 2001;63:749–63.
[7] Sandler SR, Koro W, Bonested JA, Pearce EM. Polymer synthesis and characterisation. A laboratory manual. San Diego: Academic Press; 1998.
[8] Sirisinha K, Chimdist S. Polym Test 2006;25:518–26.
[9] Garcia-Calzon JA, Diaz-Garcia ME. Sens Actuators B Chem 2006;123:1180–94.
[10] Cummins W, Duggan P, McLoughlin P. Anal Bioanal Chem 2008;391:1237–44.
[11] Holland N, Cummins W, Duggan P, McLoughlin P. Anal Bioanal Chem 2008;391:1245–53.
[12] Sellergren B, Shea KJ. J Chromatogr A 1995;690:29–39.
[13] Allender CJ, Brain KR, Heard CM. Chirality 1997;9:233–7.
[14] Umpleby RJ, Baxter SC, Rampey AM, Rushton GT, Chen Y, Shimizu KD. J Chromatogr B 2004;804:141–9.
[15] Umpleby RJ, Baxter SC, Chen Y, Shah R, Shimizu KD. Anal Chem 2001;73:4584–91.
[16] Umpleby RJ, Baxter SC, Bode M, Berch J, Shah R, Shimizu KD. Anal Chim Acta 2001;435:35–47.
[17] Lehmann M, Dettling M, Brunner H, Tovar GEM. J Chrom B 2004;804:43–50.
[18] Cacho C, Turiel E, Martin-Esteban A, Preze-Conde C, Camara C. J Chromatogr B 2004;802:347–53.
[19] Li X, Husson SM. Biosens Bioelectr 2006;22:336–48.
[20] Tamayo FG, Casillas JL, Martin-Esteban A. J Chrom A 2005;1069:173–81.
[21] Turiel E, Preze-Conde C, Martin-Esteban A. Analyst 2003;128:137–41.
[22] Kim H, Guiochon G. Anal Chem 2005;77:1708–17.
[23] Stanley BJ, Bialkaowski SE, Marshall DB. Anal Chem 1993;65:259–67.
[24] Stanley BJ, Szableski P, Chen YB, Sellergren B, Guiochon G. Langmuir 2003;19:772–8.
[25] Wei S, Jakusch M, Mizaikoff B. Anal Bioanal Chem 2007;389:423–31.
[26] Corton E, Garcia-Calzon JA, Diaz-Garcia ME. J Non-Cryst Solids 2007;353:974–80.
[27] Kim H, Spivak DA. J Am Chem Soc 2003;125:11269–75.
[28] Szabelski P, Cavazzini A, Chen YB, Sellergren B, Guiochion G, Kaczmarski K. J Chrom A 2002;964:99–111.
[29] Umpleby RJ, Rushton GT, Shah RN, Rampey AM, Bradshaw J, Berch J, et al. Macromol 2001;34:8116–52.
[30] Takeuchi T, Mukawa T, Matsui J, Higashi M, Shimiau KD. Anal Chem 2001;73:3869–74.
[31] Thoelen R, Vansweevelt R, Duchateau J, Horemans F, Haen JD, Lusten L, et al. Biosens Bioelectr 2008;23:913–8.
[32] Rampey AM, Umblepy RJ, Rushton GT, Iseman J, Shah R, Shimizu KD. Anal Chem 2004;74:1123–33.
[33] Wei S, Molinelli A, Mizaikoff B. Biosens Bioelectr 2006;21:1943–51.
[34] Dineiro Y, Menendez MI, Blanco-Lopez MC, Lobo-Castanon MJ, Miranda-Ordieres AJ, Tinon-Blanco P. Biosens Bioelectr 2006;22:364–71.
[35] Ulbricht M, Bode M, Shimizu KD. Analyst 2000;125:1261–5.
[36] Umpleby RJ, Rushton GT, Shah RN, Rampey AM, Bradshaw J, Berch J, et al. Macromol 2001;34:8446–52.
[37] Thakur AK, Munson PJ, Hunston DL, Rodbard D. Anal Biochem 1980;103:240–54.
[38] Hunston D. Anal Biochem 1975;63:99–109.
[39] Osmani Q, Hughes H, Flavin K, Hedin-Dahlstrom J, Allender CJ, Frisby J, et al. Anal Bioanal Chem 2008;391:1229–39.
[40] Jie Z, Xiwen H. Anal Chim Acta 1999;381:85–91.
[41] Mullett WM, Dirie MF, Lai EPC, Guo H. Anal Chim Acta 2000;414:123–31.
[42] Cummins W, Duggan P, McLoughlin P. Anal Chim Acta 2005;542:52–60.
[43] Cummins W, Duggan P, McLoughlin P. Biosens Bioelectr 2006;22:372–80.
[44] Joshi VP, Kulkarni MG, Mashelkar RA. J Chromatogr A 1999;849:319–30.
[45] Piletsky SA, Piletska EV, Guerrerio A, Chianella I, Karim K, Turner APF. Macromol 2004;37:5018–22.
[46] Barrett EP, Joyner L, Halenda PP. J Am Chem Soc 1951;73:373–80.
[47] Thommes M. In: Lu GQ, Zhao XS-, editors. Nonporous materials-science and engineering. London: Imperial College Press; 2004. p. 317–64.
[48] Sing KSW. Pure Appl Chem 1982;52:2201–18.
[49] Santora BP, Gange MR, Moloy KG, Radu NS. Macromol 2001;34:648–61.
[50] Guyot A. In: Sherrington D, Hodge P-, editors. Synthesis and separations using functional monomers. Wiley and Sons; 1988.
[51] Sherrington D. Chem Comm 1998:2275–86.
[52] Lu Y, Li X, Wang X, Sun P, Xing X. J Chromatogr B 2004;804:53–9.